Modulation of the Membrane Orientation and Secondary Structure of the C-Terminal Domains of Bak and Bcl-2 by Lipids†

Alejandro Torrecillas,‡ María M. Martínez-Senac,‡ Erik Goormaghtigh,§ Ana de Godos,‡ Senena Corbalán-García,‡ and Juan C. Gómez-Fernández*,‡

Departamento de Bioquímica y Biología Molecular A, Facultad de Veterinaria, Universidad de Murcia, Apartado 4021, E-30080 Murcia, Spain, and Structure and Function of Biological Membranes, Free University of Brussels, Campus Plaine CP 206/2, B1050 Brussels, Belgium

Received February 21, 2005; Revised Manuscript Received June 20, 2005

ABSTRACT: Infrared spectroscopy was used to study the secondary structure of peptides which imitate the amino acid sequences of the C-terminal domains of the pro-apoptotic protein Bak (Bak-C) and the anti-apoptotic protein Bcl-2 (Bcl-2-C) when incorporated into different lipid vesicles. Whereas β-pleated sheet was the predominant type of secondary structure of Bak-C in the absence of membranes, the same peptide adopted different structures depending on lipid composition when incorporated into membranes, with the predominance of the α-helical structure in the case of DMPC and other phospholipids, such as POPC and POPG. However, β-pleated sheet was the predominant structure in other membranes containing phospholipids with longer fatty acyl chains and cholesterol, as well as in a mixture which imitates the composition of the outer mitochondrial membrane (OMM). Similarly, Bcl-2-C adopted a structure with a predominance of intermolecularly bound pleated β-sheet in the absence of membranes, with α-helix as the main component in the presence of DMPC and POPG, but intermolecular β-sheet in the presence of EYPC and cholesterol. Using ATR-IR, it was found that the orientation of the α-helical components of both domains was nearly perpendicular to the plane of the membrane in the presence of DMPC membranes, but not in EYPC or OMM membranes. ^{2}H NMR spectroscopy of DMPC-d_{54} confirmed the transmembrane disposition of the domains, revealing that they broadened the phase transition temperature, although the order parameter of the C−D bonds was not affected, as might have been expected for intrinsic peptides. When all these results are taken together, it was concluded that the domains only form transmembrane helices in membranes of reduced thickness and that hydrophobic mismatching occurs in thicker membranes, as happens in the membrane imitating the composition of the OMM, where the peptides were partially located outside the membranes.

The Bcl-2 family members are central regulators of apoptosis that promote or inhibit cell death (*1*−*3*). These proteins are characterized by the presence of distinct conserved sequence motifs known as Bcl-2 homology (BH) domains, designated BH1, BH2, BH3, and BH4 (*1*, *2*, *4*). In general, the anti-apoptotic members (e.g., Bcl-2, Bcl-x_L, Mcl-1, and Bcl-w from mammals and Ced-9 from *Caenorhabditis elegans*) display sequence homology in all four BH domains, whereas the pro-apoptotic members (e.g., Bax, Bak, and Bok) have homologous BH1−BH3 domains. Upon activation by apoptotic stimuli, the pro-apoptotic Bcl-2 family members are capable of forming heterodimers with anti-apoptotic members. The solution structure of Bcl-x_L reveals that the BH1−BH3 domains of Bcl-x_L form an elongated hydrophobic groove, which is the docking site for the BH3 domains of pro-apoptotic binding partners (*5*). Deletion and mutagenesis studies show that the BH3 domains of pro-apoptotic members are critical for their pro-apoptotic and heterodimerization function (*6*). There is, in fact, a third subset of the pro-apoptotic members of the Bcl-2 family, collectively known as the BH3-only proteins (e.g., Bid, Bad, Bik, Bim, Bmf, Puma, Noxa, and Hrk/DP5 from mammals and Egl1 from *C. elegans*) that share sequence homology only in the BH3 domain (*7*).

Many lines of evidence suggest that anti-apoptotic Bcl-2 family members appear to function, at least in part, by interacting with antagonizing pro-apoptotic family members (*1*, *6*). Although heterodimerization between the pro-apoptotic and anti-apoptotic members regulates their respective functions, there is evidence to support the idea that anti-apoptotic proteins of the Bcl-2 family can exert their prosurvival function in a manner independent of whether they bind to the pro-apoptotic proteins. Indeed, as suggested by their structural homology to the bacterial pore-forming domains, Bcl-x_L, Bcl-2, and Bax have been shown to form ion channels in biological membranes (*8*). However, it has

† This work was supported by Grants BMC2002-00119 from Dirección General de Investigación, Ministerio de Ciencia y Tecnología (Spain), and PI-35/00789/FS/01 from Fundación Séneca (Comunidad Autónoma de Murcia, Spain). A.T. is a recipient of a postdoctoral fellowship from the Universidad de Murcia. S.C.-G. belongs to "Ramón y Cajal" Programme supported by the Ministerio de Ciencia y Tecnología and the Universidad de Murcia.

* To whom correspondence should be addressed. Telephone and Fax: +34-968364766. E-mail: jcgomez@um.es.

‡ Universidad de Murcia.

§ Free University of Brussels.

10.1021/bi0503192 CCC: $30.25
Published on Web 07/19/2005

not been possible to measure Bcl-2- or Bcl-x_L-like channels in intact cells, and it has not been confirmed in vivo whether Bcl-2-like anti-apoptotic proteins form membrane pores.

In addition to the BH domains, some members of this family possess a C-terminal domain that has a hydrophobic character and is thought to be associated with membranes, at least in some cases. It has been described that Bcl-2 (as well as Bcl-x_L) spontaneously inserts into membranes. It was hypothesized that the C-terminal α-helix of Bcl-2 serves both as a membrane-targeting signal and as a membrane anchor. This possibility has often been verified by the observation that C-terminally truncated variants of Bcl-2 (and Bcl-x_L) lose their ability to insert into membranes in vitro and in vivo, as their anti-apoptotic activity increases (*9*, *10*), and the same is true in yeast. Furthermore, these C-terminally truncated variants are unable to prevent the effects of the expression of Bax on the release of cytochrome *c* (*11*) and cell death (*11*, *12*). It has also been shown that the isolated C-terminal domain of Bcl-2 is inserted into membranes (*13*).

Recently, certain C-terminally deleted mutants of the anti-apoptotic protein Bcl-w were found to lose their anti-apoptotic function, although they are still able to bind BH3-only proteins, such as BimL and Bad, suggesting a novel role for the C-terminal residues in modulating biological activity (*14*). Prosurvival Bcl-2-related proteins, which are critical regulators of apoptosis, contain a hydrophobic groove targeted for binding by the BH3 domain of the BH3-only proteins. In this case, the groove appears to be occluded by the C-terminal residues. Binding and kinetic data suggest that the C-terminal residues of Bcl-w and Bcl-x_L modulate prosurvival activity by regulating ligand access to the groove. Binding of the BH3-only proteins, which is critical for cell death initiation, probably displaces the hydrophobic C-terminal region of Bcl-w and Bcl-x_L. Moreover, Bcl-w does not act only by sequestering the BH3-only proteins (*14*).

In the case of pro-apoptotic proteins, it is controversial whether the C-terminal domain of Bax is or is not able to insert into the membrane (*15*); however, Bak is localized in the outer mitochondrial membrane in healthy cells (*3*, *16*), and its C-terminal domain has been shown to interact with membranes (*17*).

There is a growing body of evidence that shows that lipid composition and, in particular, the presence of cholesterol in a membrane may be important for determining the localization of these peptide domains with respect to the lipid bilayer. In some cases, the presence of cholesterol has been described to alter the localization of the peptides in the membrane (*18*, *19*), inhibit their insertion (*20*−*22*), or produce aggregation in the surface of the membrane (*23*).

In this paper, we have studied the C-terminal domains of pro-apoptotic Bak and anti-apoptotic Bcl-2 proteins when they are inserted in lipid vesicles, finding that lipid composition may modulate their secondary structure and their orientation with respect to the lipid bilayer.

EXPERIMENTAL PROCEDURES

Materials. The synthetic Bcl-2 C-terminal domain peptide (Bcl-2-C) encompassed residues 217−239 of Bcl-2 (NH_3^+-^{217}LTKLLSLALVGACITLGAYLGHK^{239}-COO^-), whereas the synthetic Bak C-terminal domain peptide (Bak-C) included residues 188−211 of Bak (NH_3^+-^{188}ILNVLVVLGVVLLGQFVVRRFFKS^{211}-COO^-). The length of the C-terminal domains was selected according to the theoretical prediction calculated with the hydropathicity degree of the sequence proposed by Kyte and Doolittle (*24*), which is available in the ExPASy website (www.expasy.org) (Figure 1). Furthermore, other authors have used similar or even smaller fragments as the C-terminal domains of these proteins (*25*−*27*). Both synthetic peptides and the N-acetylated form of Bcl-2-C were purchased from Genemed (San Francisco, CA) and judged to be pure (>95%) according to HPLC and MALDI-TOF spectroscopy.

Bak:			
Theoretical:	187	PILNVLVVLGVVLLGQFVVRRFFKS	211
Bak-C:	188	ILNVLVVLGVVLLGQFVVRRFFKS	211
Bcl-2:			
Theoretical:	216	SLKTLLSLALVGACITLGAYLGHK	239
Bcl-2-C:	217	LKTLLSLALVGACITLGAYLGHK	239

FIGURE 1: Comparison of the sequences determined by the theoretical prediction and those used in this study corresponding to the C-terminal domains of Bak (Bak-C) and Bcl-2 (Bcl-2-C). The theoretical prediction was performed using the hydropathicity degree proposed by Kyte and Doolittle (*24*), available in the ExPASy website (www.expasy.org), and considering the 45 amino acid residues at the C-terminal end of each protein.

Egg yolk phosphatidylcholine (EYPC),[1] egg yolk trans-phosphatidylethanolamine (EYPE-t), cardiolipin, cholesterol (Chol), sphingomyelin (SM), 1,2-dimyristoyl-*sn*-glycero-3-phosphocholine (DMPC), 1-palmitoyl-2-oleyl-*sn*-glycero-3-phosphocholine (POPC), and 1-palmitoyl-2-oleyl-*sn*-3-phospho-*rac*-glycerol (POPG) were purchased from Avanti Polar Lipids, Inc. (Alabaster, AL). The outer mitochondrial membrane (OMM) was prepared with 45% PC, 21% PE, 13% PI, 3.5% PG, 3% cardiolipin, 4.5% SM, and 10% Chol (molar percentages), as previously described (*28*). 2,2,2-Trifluoroethanol (TFE) and tetrahydrofuran (THF) were from Sigma (Madrid, Spain), and all other reagents used in this work were analytical grade. Both deuterium water and deuterium-depleted water were from Aldrich (Madrid, Spain). Water was twice distilled and deionized using a Millipore system from Millipore Ibérica (Madrid, Spain).

Fourier Transform Infrared Spectroscopy (FT-IR). The infrared spectra were obtained using a Bruker Vector 22 Fourier transform infrared spectrometer equipped with a liquid nitrogen-cooled MCT detector. Each spectrum was obtained after equilibrating the samples at 20 °C for 20 min in the infrared cell by collecting 500 interferograms with a nominal resolution of 4 cm^{-1} and triangular apodization using the sample shuttle accessory to average background spectra between sample spectra over the same time period. The sample chamber of the spectrometer was continuously purged with dry air to prevent atmospheric water vapor from obscuring the bands of interest.

[1] Abbreviations: ATR-IR, attenuated total reflection infrared spectroscopy; Chol, cholesterol; DMPC, 1,2-dimyristoyl-*sn*-glycero-3-phosphocholine; EYPC, egg yolk phosphatidylcholine; EYPE-t, egg yolk trans-phosphatidylethanolamine; FT-IR, Fourier transform infrared spectroscopy; LUVs, large unilamellar vesicles; MLVs, multilamellar vesicles; OMM, outer mitochondrial membrane; PC, phosphatidylcholine; PE, phosphatidylethanolamine; PG, phosphatidylglycerol; PI, phosphatidylinositol; POPC, 1-palmitoyl-2-oleoyl-*sn*-glycero-3-phosphocholine; POPG, 1-palmitoyl-2-oleoyl-*sn*-3-phospho-*rac*-glycerol; T_c, transition temperature; TFE, 2,2,2-trifluoroethanol; THF, tetrahydrofuran.

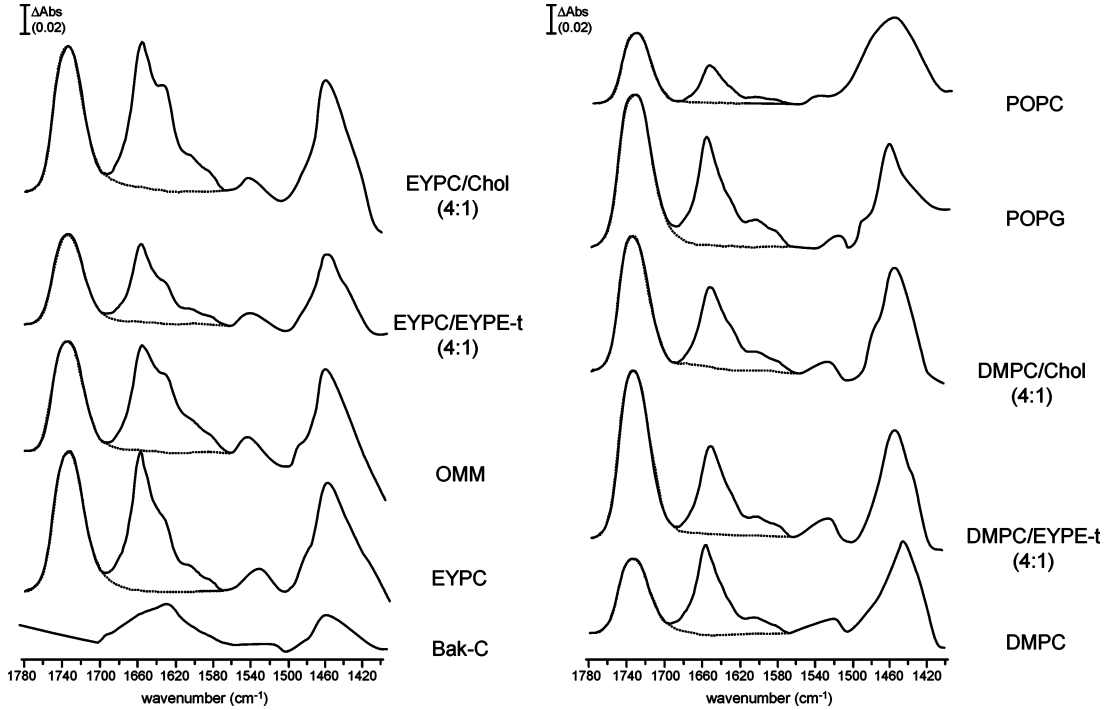

FIGURE 2: FT-IR spectra of Bak-C (solid lines) in D_2O buffer [10 mM Hepes (pD 7.4) and 0.1 mM EDTA] at 20 °C, and in the presence of different lipid mixtures, in the range of 1800−1400 cm^{-1}, where amide I′, amide II, and amide II′ regions can be seen. The parameters corresponding to the fitted component bands are shown in Table 1. The spectra of each lipid mixture alone are also depicted as dashed lines.

Samples were prepared as previously described (*13*, *17*, *28*) with 0.18 μmol of peptides dissolved in TFE and 1.8 or 18 μmol of total lipid (i.e., 1:10 or 1:100 peptide:lipid molar ratio, respectively) in a chloroform/methanol mixture (1:1, v/v). These lipid/peptide mixtures were dried twice under a stream of oxygen-free N_2, and then the last traces of solvents were removed by a further 3 h evaporation under high vacuum. Samples were then hydrated in 100 μL of D_2O buffer [10 mM Hepes (pD 7.4) and 0.1 mM EDTA] and dispersed for 1 h with vigorous vortexing in the liquid−crystalline phase, i.e., above the transition temperature of the lipid mixture, to produce multilamellar vesicles (MLVs). Next, the samples were centrifuged at 13200*g* for 30 min. The lipid phase at the top of the solution and the supernatant phase were separated from the pellet and centrifuged again to obtain the highest degree of lipid phase separation from the supernatant. The lipid phase containing bound peptide (25 μL) was then transferred to a Specac 20710 cell equipped with CaF_2 windows and 25 μm Teflon spacers (Specac, Kent, U.K.). With this procedure, the peptide signal detected by FT-IR arose only from the peptide bound to the lipid. The spectra of the lipid mixtures alone were also recorded and showed that they did not affect the amide I′ band (1700−1600 cm^{-1}) (see Figures 2 and 3). The solvent contribution was eliminated interactively by subtracting the pure buffer spectrum from the sample spectrum, using the Grams/32 software (Galactic Industries Corp., Salem, NH). Data treatment and band decomposition were performed as previously described (*13*, *17*, *28*−*32*). The fractional areas of the bands in the amide I′ region were calculated from the final fitted band areas. The procedure used here to quantitatively calculate the secondary structure is usually assumed to have an error of ∼1% (*32*), and in this paper, we have assumed it to be 1−2%, as deduced from the comparison of at least three independent experiments and the repetition of the fitting procedure by three different persons. Therefore, we will assume as being significantly different changes in the structural components of >4%.

Attenuated Total Reflection Infrared Spectroscopy (ATR-IR). This method is one of the most powerful tools for recording infrared spectra of biological materials, especially biological membranes (*33*, *34*). ATR-IR requires small quantities of sample (only a few micrograms) and gives information about the orientation of various parts of the molecule under study to be evaluated in an oriented system, allowing the simultaneous study of the structure of lipids and proteins in intact biological membranes without the addition of foreign probes (*35*).

The ATR-IR method is based on the fact that infrared light absorption is maximal if the dipole transition moment is parallel to the electric field component of the incident light (*35*). In an ordered membrane deposited on the internal reflection element surface (ATR plate), all the molecules and, therefore, the transition dipole moments within the membrane molecules have the same orientation with respect to a normal to the ATR plate surface (*34*). It is therefore possible to detect changes in the orientation of a number of chemical bonds belonging to lipids and proteins (*34*, *36*, *37*). By measuring the spectral intensity while turning the incident light electric field orientation with a polarizer, we were able to obtain more information about the orientation of the dipoles. In fact, all the orientation information is contained in the dichroic ratio R^{ATR}, which is the ratio between the integrated absorbance of a band measured with a parallel polarization of the incident light ($A_{||}$) and the absorbance measured with a perpendicular polarization of the incident light ($A_{\perp}$):

$$R^{ATR} = A_{||}/A_{\perp}$$

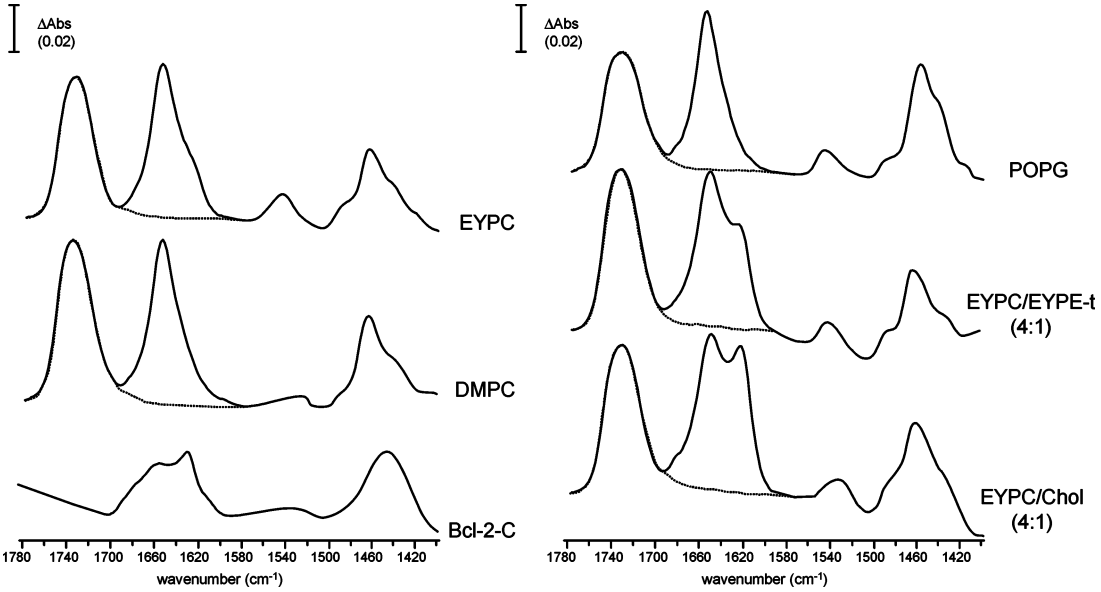

FIGURE 3: FT-IR spectra of Bcl-2-C (solid lines) in D_2O buffer [10 mM Hepes (pD 7.4) and 0.1 mM EDTA] at 20 °C, and in the presence of different lipid mixtures, in the range of 1800−1400 cm^{-1}, where amide I′, amide II, and amide II′ regions can be seen. The parameters corresponding to the fitted component bands are shown in Table 2. The spectra of each lipid mixture alone are also depicted as dashed lines.

The dichroic spectrum is the difference between the spectra recorded with parallel and perpendicular polarizations. A larger absorbance for the parallel polarization (upward deviation on the dichroic spectrum) indicates a dipole oriented preferentially near the normal of the ATR plate. Conversely, a larger absorbance for the perpendicular polarization (downward deviation on the dichroic spectrum) indicates a dipole oriented approximately parallel to the ATR plate. In this calculation, the perpendicular spectrum is multiplied by a factor before subtraction to take into account the differences in the relative power of the evanescent fields. This factor is the dichroic ratio for an isotropic distribution of the dipoles (R^{iso}), which is difficult to find in practice, as all the molecules composing the film are oriented with respect to the interface, including water. Bechinger et al. (*38*) suggested that as the C═O orientation is on average close to the magic angle with respect to the bilayer normal, the dichroic ratio of the band at 1738 cm^{-1}, i.e., ν(C═O), provides a good estimation of R^{iso}.

The presence of residues containing secondary structures other than α-helix introduces some changes into the previous analysis, and we have to consider the α-helix dichroic ratio, R^{α}:

$$R^{\alpha} = A_{||}/A_{\perp} = \frac{R^{ATR} - \frac{R^{ATR}+2}{2R^{iso}+1}(1-x)}{1 - \frac{1}{R^{iso}}\frac{R^{ATR}+2}{2R^{iso}+1}(1-x)}$$

where R^{ATR} is the amide I dichroic ratio, R^{iso} is the dichroic ratio of the band at 1738 cm^{-1} (C═O band), and x is the fraction of α-helix component in the protein sample. The angles between the amide I dipole and the helix main axis that are reported in the literature vary between 20 and 40° (*33*, *36*, *37*).

Spectra were recorded at 20 °C with incident light, which is polarized parallel or perpendicular relative to the incidence plane by using a ZnSe polarizer (Specac) on a Bruker Vector 22 Fourier transform infrared spectrometer equipped with a liquid nitrogen-cooled MCT detector. The internal reflection element was a germanium ATR plate (Specac) (52 mm × 20 mm × 2 mm) with an aperture angle of 45°. The crystal surface was rendered hydrophilic by washing it with an alkaline detergent, rinsing it with distilled water, and washing it with methanol and chloroform. A total of 500 scans were accumulated for each spectrum with a nominal resolution of 4 cm^{-1}. The background spectrum was a single-beam spectrum collected from an empty ATR crystal. The spectrometer was continuously purged with dry air to clean out the water vapor absorption. The remaining interference of water vapor absorption was eliminated by subtracting from these spectra a separately measured water vapor spectrum.

Samples were prepared as previously stated (*39*) with a peptide:lipid molar ratio of 1:10. In this sense, a solution of 0.295 μmol of the corresponding lipid mixture in a chloroform/methanol mixture (1:1, v/v) was added to 0.0295 μmol of peptide (80 μg) dissolved in TFE. Samples were then dried under N_2 and stored in a vacuum for 1 h. Then, 200 μL of TFE and 20 μL of Cl_4C were added, and oriented films were obtained by applying this solution onto one side of a germanium plate and drying it under a stream of N_2 (*38*, *39*). The last traces of solvents were removed by a further 3 h evaporation under high vacuum. The crystal was placed in the liquid sample holder with connections to allow a stream of air (wet in D_2O) to hydrate its surface for 15 min before collection of spectra.

^{2}H NMR Spectroscopy. Samples for ^{2}H NMR were prepared at a peptide:lipid molar ratio of 1:14. Organic solutions containing 10.92 μmol of DMPC-d_{54} (8 mg) were mixed with 0.84 μmol of each peptide (2.3 mg of Bak-C and 2.0 mg of Bcl-2-C) dissolved in TFE. A sample including only 8 mg of DMPC-d_{54} was also prepared as a reference. Samples were dried under a stream of oxygen-free nitrogen, and then the last traces of solvents were removed by a further 3 h evaporation under high vacuum. Then, 200 μL of TFE

Table 1: FT-IR Parameters of the Amide I′ Band Components of Bak-C in D_2O Buffer [10 mM Hepes (pD 7.4) and 0.1 mM EDTA] at 20 °C, and in the Presence of EYPC, OMM, EYPC/EYPE-t (4:1), EYPC/Chol (4:1), DMPC, DMPC/EYPE-t (4:1), DMPC/Chol (4:1), POPG, and POPC MLVs[a]

	Bak-C		EYPC		OMM		EYPC/EYPE-t		EYPC/Chol	
assignment	position[b] (cm^{-1})	area[c]	position[b] (cm^{-1})	area[c]	position[b] (cm^{-1})	area[c]	position[b] (cm^{-1})	area[c]	position[b] (cm^{-1})	area[c]
turns	1679	10	1675	10	1675	6	1675	10	1675	7
α-helix	1658	33	1658	48	1656	45	1656	49	1656	47
random	1645	8	1645	3	1644	2	1644	3	1645	2
β-pleated sheet	1627	49	1635	39	1632	47	1631	38	1632	44
	DMPC		DMPC/EYPE-t		DMPC/Chol		POPG		POPC	
assignment	position[b] (cm^{-1})	area[c]	position[b] (cm^{-1})	area[c]	position[b] (cm^{-1})	area[c]	position[b] (cm^{-1})	area[c]	position[b] (cm^{-1})	area[c]
turns	1676	12	1678	7	1678	6	1678	9	1676	7
α-helix	1657	58	1657	59	1657	57	1657	58	1656	59
random	1644	5	1642	3	1642	4	1642	4	1642	6
β-pleated sheet	1633	25	1632	31	1632	33	1632	29	1632	29

[a] Samples were prepared at a lipid:peptide molar ratio of 10:1 (see Experimental Procedures). [b] Peak position of the amide I′ band components. [c] Percentage area of the amide I′ band components. The area corresponding to side chain contributions located at 1600−1615 cm^{-1} has not been considered.

was added, and the samples were vortexed vigorously and dried again, as described previously. MLVs were formed by incubating the dried samples in 200 μL of buffer containing 10 mM Hepes (pH 7.4) and 0.1 mM EDTA, in the liquid−crystalline phase, i.e., above the transition temperature of the lipid mixture, for 1 h with vigorous vortexing. This buffer was prepared using deuterium-depleted water (Aldrich Chemical Co., Milwaukee, WI).

^2H NMR spectra were acquired in a Bruker Avance 400 spectrometer at 61.54 MHz using the standard quadrupole echo sequence (*40*). The spectral width was 150 kHz, with a 10 μs 90° pulse, a 40 μs pulse spacing, a 3.35 μs dwell time, a 1 s recycle time, a 50 Hz line broadening, and accumulation of 2000 transients. Spectra were recorded at different temperatures, above and below the transition temperature (T_c) of the pure phospholipid, as indicated in each case. Spectra were de-Paked by numerical deconvolution with the software supplied by Bruker. The de-Paked spectra correspond to the spectra that would be obtained from a planar membrane with its bilayer normal aligned parallel to the applied static magnetic field, enhancing resolution and facilitating analysis of individual spectral peaks (*41*). These spectra were compared with the original spectra to ensure that the relevant features were maintained through the de-Paking process.

RESULTS

The interaction of Bak-C and Bcl-2-C with membranes was studied by using different spectroscopic techniques with the aim of revealing how membrane lipid composition influences the secondary structure of the peptides and their orientation in the membrane, and also how the peptides affect lipid dynamics.

Infrared Spectroscopy of Bak-C in the Presence of Different Membrane Compositions. The amide I′ band of the infrared spectrum of Bak C-terminal domain peptide in D_2O buffer showed a maximum at 1636 cm^{-1} (Figure 2 and Supporting Information), indicating the predominance of β-sheet in its secondary structure (*42*−*45*). The corresponding parameters, band position, percentage area, and assignment of each spectral component are shown in Table 1. The component with the maximum contribution (49%) was located at 1627 cm^{-1}, and probably corresponds to intramolecular C═O vibrations of peptidyl bonds within β-pleated sheets (*42*−*45*). The component at 1658 cm^{-1} amounted to 33%, and can be attributed to α-helix (*44*, *45*), while the components at 1679 and 1690 cm^{-1} (10%) can be assigned to turns or to antiparallel β-structures (*46*−*49*). Finally, the band located at 1645 cm^{-1} (3%) can be attributed to nonstructured conformations, including open loops (*32*, *46*, *47*).

The infrared spectra were quite different when Bak-C was resuspended in the presence of MLVs with different lipid compositions. As shown in Figure 2, there is a clear shift of the maxima toward a higher wavenumber (1656−1658 cm^{-1}), indicative of the predominance of α-helical structures. However, it is striking that membrane lipid composition determined the amide I′ contour and hence the secondary structure of Bak-C, so the shoulder appearing at ∼1631−1635 cm^{-1} and which indicates the presence of β-pleated sheet was more important with certain lipid mixtures.

When Bak-C was incorporated into EYPC vesicles, the band decomposition of the infrared spectrum (Figure 2, Table 1, and Supporting Information) showed that the main component (48%) appeared at 1658 cm^{-1} (α-helix), while the band at 1635 cm^{-1} (β-sheet) represented 39%. When the composition of the membrane was designed to imitate that of the OMM, the structure that Bak-C adopted was clearly different from that observed with EYPC (Figure 2, Table 1, and Supporting Information). In this case, the main component (47%) was located at 1632 cm^{-1}, indicating the presence of β-pleated sheet, whereas the band corresponding to α-helix (1656 cm^{-1}) amounted to 45%.

It can be seen in Table 1 that the other lipid compositions that were tested produced secondary structures of Bak-C with variations in the predominance of α-helix or β-pleated sheet. When EYPE-t was added to EYPC at a 1:4 molar ratio, the structure did not change with respect to pure EYPC (within experimental error), but when cholesterol was added to EYPC at the same molar ratio, the structure was identical (within experimental error) to that seen with the mixture imitating the OMM (Figure 2 and Table 1). This result shows that the addition of cholesterol influenced the increase in β-pleated sheet (from 39% in EYPC vesicles alone to 44%).

The effect of DMPC was different (Figure 2 and Table 1), since, in its presence, Bak-C exhibited a high α-helix (58%) and a low β-pleated sheet (25%) content. The different composition of the fatty acyl chains between EYPC and DMPC, both in the number of insaturations and in chain lengths, must be involved in this structure change. No changes were observed when comparing spectra of Bak-C with DMPC vesicles at different temperatures (10 and 30 °C) (not shown), indicating that the presence of gel or fluid phases did not influence the secondary structure of Bak-C. The addition of EYPE-t or cholesterol to DMPC resulted in an increase in the β-pleated sheet content to 31 or 33%, respectively, with some decreases in β-turn content.

In the presence of a negatively charged phospholipid like POPG, the secondary structure of Bak-C was very similar to that obtained in DMPC vesicles. The α-helical structure (1657 cm^{-1}) was predominant with 58%, whereas β-pleated sheet (1632 cm^{-1}) amounted to only 29% (Figure 2 and Table 1). This result indicates that the negative charge was not important in determining the secondary structure of Bak-C. Finally, in the presence of POPC (Figure 2 and Table 1), the results were the same as with POPG (within experimental error), and very similar to those obtained with DMPC, indicating again that the negative charge was not important in determining the secondary structure of Bak-C. It is interesting that EYPC and POPC membranes have considerably different effects on the secondary structure of Bak-C. In this sense, the content in α-helix was higher in POPC membranes, whereas the percentage of β-pleated sheet was higher in EYPC vesicles. These differences may be explained by the differences in the fatty acyl chain length and unsaturation.

Bak-C was prepared in the presence of EYPC or DMPC at a peptide:lipid molar ratio of 1:100 to test whether the aggregation was favored by a high peptide concentration. The spectra were very similar to those obtained with a peptide:lipid molar ratio of 1:10. Band decomposition showed that the calculated percentage of each secondary structure component was the same, within experimental error, i.e., with differences of less than 4% (see Supporting Information).

Infrared Spectroscopy of Bcl-2-C in the Presence of Different Membrane Compositions. The maximum of the amide I′ band of the infrared spectrum of the Bcl-2-C peptide in D_2O buffer was located at 1622 cm^{-1} (Figure 3 and Supporting Information), a frequency which indicates the presence of aggregated peptide molecules with intra- or intermolecular hydrogen bonding and which is usual in thermally denatured proteins (*13*, *29*, *30*, *50*, *51*). The corresponding parameters, band position, percentage area, and assignment of each spectral component of the amide I′ region are shown in Table 2. The component with the maximum contribution (35% of the total area) was located at 1649 cm^{-1}, which corresponds to α-helix. The component at 1620 cm^{-1} (28%) can be assigned to aggregated extended structures (*13*, *29*, *30*, *50*, *51*). The band at 1632 cm^{-1} (17%) can be attributed to β-sheets, while the high-frequency components at 1668 (19%) and 1681 cm^{-1} (4%) can be assigned to turns or β-structures.

Bcl-2-C was incorporated in similar lipid mixtures to Bak-C. In this case, the infrared spectrum was quite different when Bcl-2-C was resuspended in the presence of MLVs of EYPC, the maximum of the amide I′ band now being centered at 1654 cm^{-1}, indicative of a predominantly α-helical structure (Figure 3, Table 2, and Supporting Information) and representing 57%. The band at 1640 cm^{-1}, which can be assigned to unstructured conformations including open loops, amounted to 13%. The component at 1633

Table 2: FT-IR Parameters of the Amide I′ Band Components of Bcl-2-C in D_2O Buffer [10 mM Hepes (pD 7.4) and 0.1 mM EDTA] at 20 °C (*14*), and in the Presence of DMPC, POPG, EYPC, EYPC/EYPE-t (4:1), and EYPC/Chol (4:1) MLVs[a]

	Bcl-2-C	
assignment	position[b] (cm^{-1})	area[c]
turns	1681	4
turns	1668	19
α-helix, random	1649	35
β-sheet	1632	17
aggregation	1620	28
	EYPC	
assignment	position[b] (cm^{-1})	area[c]
turns	1684	3
turns	1673	7
α-helix	1654	57
random	1640	13
β-sheet	1633	9
aggregation	1622	11
	DMPC	
assignment	position[b] (cm^{-1})	area[c]
turns	1685	5
turns	1674	7
α-helix	1654	65
random	1639	12
β-sheet	1632	6
aggregation	1625	5
	POPG	
assignment	position[b] (cm^{-1})	area[c]
turns	1684	4
turns	1674	8
α-helix	1656	66
random	1641	12
β-sheet	1633	5
aggregation	1625	5
	EYPC/Chol	
assignment	position[b] (cm^{-1})	area[c]
turns	1684	4
turns	1673	4
α-helix	1653	48
random	1639	7
β-sheet	1633	6
aggregation	1623	28
	EYPC/EYPE-t	
assignment	position[b] (cm^{-1})	area[c]
turns	1683	4
turns	1674	5
α-helix	1653	58
random	1639	6
β-sheet	1633	6
aggregation	1623	21

[a] Samples were prepared at a lipid:peptide molar ratio of 10:1 (see Experimental Procedures). [b] Peak position of the amide I′ band components. [c] Percentage area of the amide I′ band components. The area corresponding to side chain contributions located at 1600−1615 cm^{-1} has not been considered.

cm^{-1}, which can be attributed to intramolecular C═O vibrations of β-sheets, was 9%, while the high-frequency components at 1673 and 1684 cm^{-1} (turns or β-structures) amounted to 7 and 3%, respectively. Finally, the component at 1623 cm^{-1}, which probably arose from aggregated extended structures, as in the sample containing peptide without lipid, was much smaller, representing only ~11% of the total area of the amide I′ band. This result indicates that most of the peptide aggregates disappeared in the presence of the phospholipid.

Figure 3 and Table 2 also show that other lipid compositions of model membranes similarly favored a conformation with a predominance of α-helix, as was the case with DMPC, where α-helical structures (1654 cm^{-1}) amounted to 65%; on the other hand, β-sheet (1633 cm^{-1}) was 6%, and only 5% corresponded to aggregation (1625 cm^{-1}). As with Bak-C, the spectra obtained at different temperatures were compared in the presence of DMPC (10 and 30 °C), and no changes were observed (not shown), indicating again that the presence of gel or fluid phases did not change the secondary structure. In the presence of POPG, the secondary structure of Bcl-2 was very similar to that obtained in DMPC vesicles (within experimental error), with the α-helical component as the predominant one. This result indicates that negative charge was not important in determining the secondary structure of Bcl-2-C.

The pattern was different, however, when the peptide was incorporated in an EYPC/cholesterol mixture (4:1 molar ratio) (Figure 3, Table 2, and Supporting Information). In this case, the α-helical component (1653 cm^{-1}) represented 48%; β-pleated sheet (1633 cm^{-1}) was 6%, and the content of aggregated extended structures (1623 cm^{-1}) increased to 28%, compared with the structure observed in EYPC vesicles (11%). Although the presence of cholesterol produced the highest increase in the level of aggregation, the EYPC/EYPE-t membrane (4:1 molar ratio) also induced the formation of aggregation in Bcl-2-C, with 58% α-helix (1653 cm^{-1}), 6% β-pleated sheet (1633 cm^{-1}), and 21% corresponding to aggregation (1623 cm^{-1}) (Figure 3 and Table 2).

The secondary structure of Bcl-2-C in the presence of a lipid mixture corresponding to the OMM was identical (within experimental error) to that found in the presence of EYPC (ref *13* and data not shown).

As mentioned above for Bak-C, Bcl-2-C was prepared in the presence of EYPC or DMPC at a peptide:lipid molar ratio of 1:100, to test the possibility that the aggregation could be favored by a high peptide concentration. The spectra were very similar to those obtained with a peptide:lipid molar ratio of 1:10. When band decomposition was carried out, the calculated percentage of each secondary structure component was the same, within experimental error, i.e., with differences of <4% (see Supporting Information).

Furthermore, the N-acetylated form of Bcl-2-C was used to check whether the peptide terminal charge influenced the secondary structure results. This modified peptide was prepared in the presence of EYPC or DMPC at a peptide:lipid molar ratio of 1:10, and no significant differences were observed compared with the spectra obtained with Bcl-2-C or after the calculation of the secondary structure component percentages (see Supporting Information). These results confirmed that the terminal charge of the peptides did not influence the secondary structure results that were obtained. Samples with the N-acetylated form of Bcl-2-C and DMPC or EYPC at a peptide:lipid molar ratio of 1:100 were also recorded, and the spectra and the percentages of secondary structure components showed no significant differences (not shown for the sake of brevity).

Orientation of Bak-C and Bcl-2-C. The orientations of these peptides were investigated in the presence of three different membrane compositions: EYPC, OMM, and DMPC (Figures 4 and 5 and Table 3). The orientation of the membranes was assessed by means of the antisymmetric and symmetric vibrations of lipid methylene C−H bonds that can be observed at ~2920 and ~2850 cm^{-1}, respectively (Table 3). These methylene bonds are perpendicular to the molecular axis of a fully extended hydrocarbon chain, and thus, measurements of the dichroism of absorbance of infrared light can provide information about the order and orientation of the membrane sample relative to the germanium crystal. Table 3 shows calculations on R^{ATR} (2920 cm^{-1}), with higher values for samples containing Bcl-2-C than for samples containing Bak-C for the same phospholipid, except with DMPC, indicating that Bcl-2-C has a stronger disordering effect on the membranes. Nevertheless, all the systems were ordered, as indicated by the order parameters (S_L) oscillating between 0.292 and 0.707, and the angles formed with the plane of the bilayer, which varied between 26.2 and 43.4° (*36*, *37*, *39*, *52*−*56*). The order parameters were maxima in the case of DMPC, and as a consequence, the angles formed with the plane of the bilayer were minimal, 26.2° in the case of Bcl-2-C and 28.9° for Bak-C. More disorder was observed for EYPC, with angles of 43.4° (Bcl-2-C) and 41.0° (Bak-C), probably due to the presence of gauche isomers, as was also the case for OMM with 36.9° (Bcl-2-C) and 31.6° (Bak-C). Very similar results were obtained for the R^{ATR} of the C−H symmetric vibration at 2850 cm^{-1} (Table 3). These values are similar to those described in previous works for well-oriented membranes (*39*, *52*−*56*). Since the membranes were oriented on the germanium crystal, it was then possible to study the orientation of the peptides inserted in them.

Information about the orientation of an α-helix can be obtained by recording ATR-IR peptide spectra with polarized light, provided that the peptides are oriented with respect to the internal reflection element. Figure 4 shows the 90° ($A_{||}$) and 0° ($A_{\perp}$) polarization spectra of the Bak-C peptide coupled to different types of lipid mixtures, as well as the difference dichroic spectra ($A_{||} - R^{iso}A_{\perp}$), obtained using the (C═O) dichroic ratio as R^{iso} (*36*, *38*). As can be observed in Figure 4, the polarization difference spectra showed positive deviation in the amide I′ band (1600−1700 cm^{-1}) in all three cases, indicating an orientation of the amide I′ dipole parallel to the lipid acyl chains, although it was higher in the cases of DMPC and EYPC and lower in the presence of OMM. In the case of Bak-C, the calculated dichroic ratio R^{α} in the presence of EYPC (48% of α-helix) was 1.555 and corresponded to an angle of 54° between the α-helix of Bak-C and a normal to the germanium plate, whereas with OMM (45% of α-helix), the dichroic ratio R^{α} was 1.364 and the angle 54° (Table 3). Finally, when the peptide was incorporated in DMPC vesicles (58% of α-helix), the dichroic ratio R^{α} was 2.512 and the angle 22° (Table 3). The dichroic ratio for the amide I′ region of this last sample and that

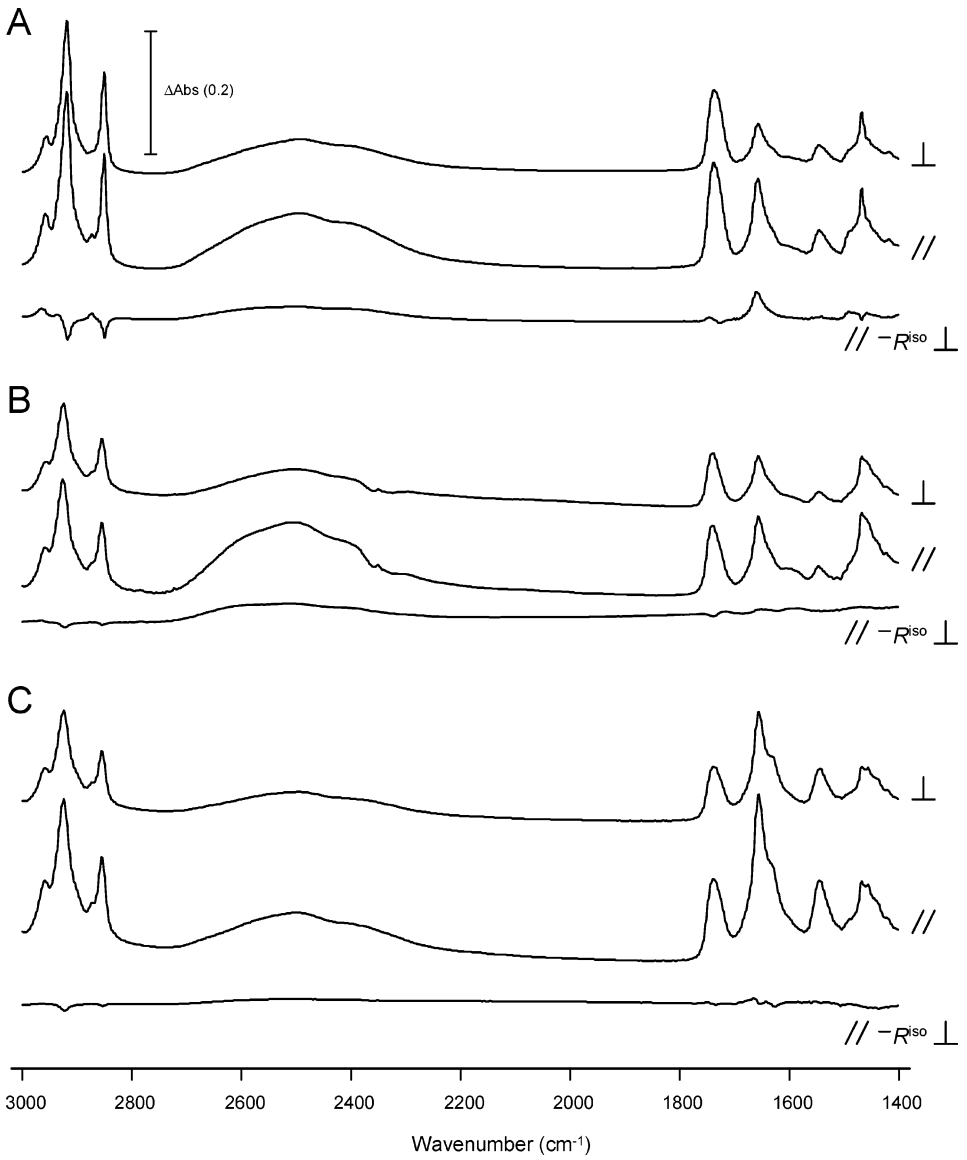

FIGURE 4: ATR-FT-IR spectra of Bak-C in the presence of DMPC (A), OMM (B), and EYPC (C), at 20 °C for parallel ($A_{||}$) and perpendicular ($A_{\perp}$) orientations of the polarizer. Difference dichroic spectra were obtained as parallel minus perpendicular spectra after multiplication of the perpendicular spectra by the dichroic ratio ($A_{||} - R^{iso}A_{\perp}$; see the text). All spectra are shown in the same scale, except the dichroic spectra whose intensity has been doubled for a better representation. The ATR-FT-IR parameters are given in Table 3.

calculated taking into account the α-helical content (R^{α}) and the angle derived from them are in the range obtained for several oriented peptides and proteins (*34*−*36*, *38*). The angles calculated for all the samples were obtained with an order parameter of 1 describing the orientation of the membrane plane with respect to the germanium plate and a value of 27° for the angle between the C═O dipole and the helix axis. If this angle were 39°, the calculated angles between the α-helix and the normal to the plate would be very similar (54° in the case of EYPC and OMM and 21° in the case of DMPC) (Table 3). We note that the angles mentioned above are the maximum possible angle, because values of <1 for the order parameter would decrease the calculated helix−axis membrane normal angle. It should be kept in mind that this technique does not discriminate between a fixed uniaxial orientation and the mean of two (or more) populations with different orientations corresponding to an average oblique orientation.

In the case of Bcl-2-C, Figure 5 shows the spectra parallel to the membrane surface ($A_{||}$) and perpendicular to it ($A_{\perp}$), together with the difference dichroic spectra ($A_{||} - R^{iso}A_{\perp}$) obtained as described above. The positive sign of the amide I′ in the difference spectra indicated the transmembrane character of the peptides under the three lipid mixtures studied, although, given the sizes of the peaks, the orientation must be better in the case of DMPC. Table 3 shows that in the presence of EYPC vesicles (57% α-helix), the calculated dichroic ratio R^{α} of 1.935 corresponds to an angle of 46° between the α-helix of Bcl-2-C and a normal to the germanium plate, whereas with OMM (68% α-helix), the dichroic ratio R^{α} was 1.590 and the angle 49°. When the peptide was incorporated into DMPC vesicles (65% α-helix), the calculated dichroic ratio R^{α} was 2.838 and the angle 10°. Once more, the dichroic ratios for the amide I′ region and R^{α} for this last sample, and also the angle derived from them, are in the range obtained for several oriented peptides and proteins (*34*−*36*, *38*). The results calculated for all the samples were obtained again with an order parameter of 1 and a value of 27° for the angle between the C═O dipole and the helix axis. When the calculation was carried out with

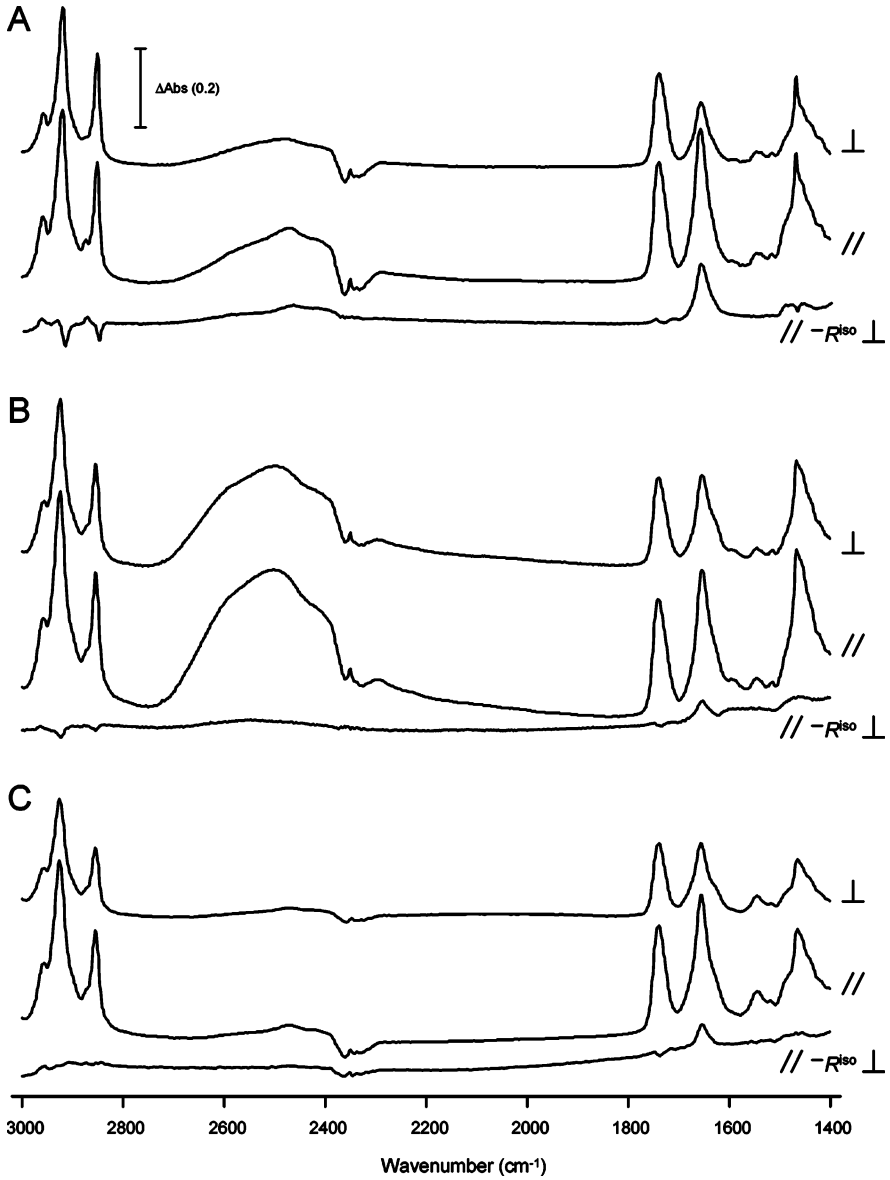

FIGURE 5: ATR-FT-IR spectra of Bcl-2-C in the presence of DMPC (A), OMM (B), and EYPC (C), at 20 °C for parallel ($A_{||}$) and perpendicular ($A_{\perp}$) orientations of the polarizer. Difference dichroic spectra were obtained as parallel minus perpendicular spectra after multiplication of the perpendicular spectra by the dichroic ratio ($A_{||} - R^{iso}A_{\perp}$; see the text). All spectra are shown in the same scale, except the dichroic spectra whose intensity has been doubled for a better representation. The ATR-FT-IR parameters are shown in Table 3.

Table 3: ATR-FT-IR Data of Bcl-2-C and Bak-C in Different Lipid Mixtures

	Bcl-2-C			Bak-C		
	EYPC	OMM	DMPC	EYPC	OMM	DMPC
R^{ATR} (2920)	1.561	1.357	1.100	1.483	1.217	1.154
S_L	0.292	0.459	0.707	0.353	0.588	0.650
θ (deg)	43.4	36.9	26.2	41.0	31.6	28.9
R^{ATR} (2850)	1.625	1.406	1.071	1.522	1.296	1.121
S_L	0.244	0.416	0.738	0.322	0.513	0.684
θ (deg)	45.2	38.6	24.7	42.2	34.7	27.3
R^{iso} (C═O)	1.558	1.418	1.207	1.535	1.352	1.269
R^{ATR} (amide I)	1.838	1.554	2.250	1.549	1.360	2.012
R^{α} (%)	1.935 (57%)	1.590 (68%)	2.838 (65%)	1.555 (48%)	1.364 (45%)	2.512 (55%)
θ (deg) ($\alpha = 27°$)	46	49	10	54	54	22
θ (deg) ($\alpha = 39°$)	40	45	10	54	54	21

an helix axis−C═O dipole angle of 39°, the results were very similar, giving slightly smaller angles (40° in the case of EYPC, 45° in the case of OMM, and 10° in the case of DMPC).

^{2}H NMR Study of the Interaction of Bak-C and Bcl-2-C with Perdeuterated DMPC. These peptides were incorporated at a 1:14 peptide:lipid molar ratio. The effect of the peptides on acyl chain order was characterized by ^{2}H NMR. Figure

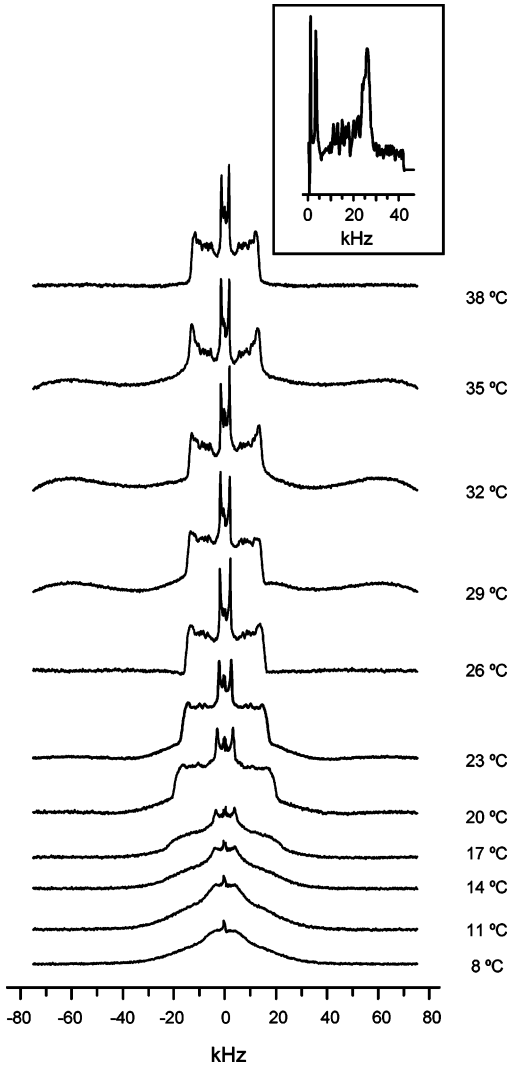

FIGURE 6: ^{2}H NMR spectra of DMPC-d_{54} vesicles in the presence of Bak-C (14:1 molar ratio), as a function of temperature. Temperatures are shown on the right-hand side of each spectrum. The inset shows the de-Paked spectrum at the highest temperature, i.e., 38 °C.

6 depicts the spectra at different temperatures of the Bak-C/DMPC-d_{54} mixture (1:14 molar ratio), from 8 to 38 °C. At low temperatures, below the transition temperature (T_c), the spectra were powder patterns characteristic of a gel phase (*57*). At temperatures of ≥20 °C, the spectra corresponded to a fluid-phase bilayer and were axially symmetric with some resolved quadrupole splittings arising from methylene segments in the acyl chains. These spectra were nearly identical to the spectra observed after the incorporation of Bcl-2-C to DMPC-d_{54} (1:14 molar ratio), and to those corresponding to pure DMPC-d_{54} (not shown), although in this last case the transition temperature was observed at 23 °C.

Since not all the individual methylene signals were completely resolved in these powder spectra, the spectra above the transition temperature were transformed into oriented ones by means of the de-Paking procedure. The de-Paked spectrum of the Bak-C/DMPC-d_{54} mixture at the highest temperature, i.e., 38 °C, is shown in Figure 6 (inset). The quadrupole splittings ($\Delta\nu^i$), the distances between the pairs of symmetric peaks, are related to the order parameters S^i_{CD} of the various CD_2 acyl chain segments according to the equation

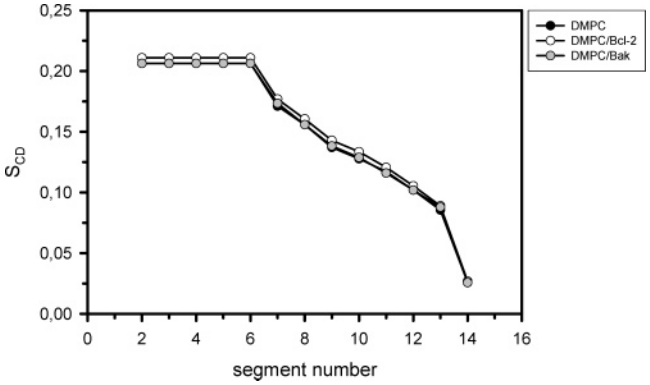

FIGURE 7: Dependence of order parameter S_{CD} on the segment number of the ^{2}H NMR samples: DMPC-d_{54} (black circles), DMPC-d_{54} and Bak-C (gray circles), and DMPC-d_{54} and Bcl-2-CTD (white circles). The calculation was made at the highest temperature, i.e., 38 °C.

$$\Delta\nu^i = {}^3/_4(e^2Qq/h)S^i_{CD}$$

where e^2Qq/h is the quadrupole coupling constant, 167 kHz (*58*). The order parameter is higher in the carbon segments next to the glycerol backbone and continuously decreases along the acyl chain toward the terminal methyl group. This gives rise to the peak pattern shown in Figure 6 (inset) consisting of eight Pake doublets, with the outermost peak pair corresponding to the plateau of superimposed peaks from carbon segments 2−6 (*59*, *60*) and the innermost pair of peaks representing the terminal methyls. As can be observed in Figure 7, the S_{CD} order parameters were not noticeably changed for any carbon segment by the addition of either Bak-C or Bcl-2-C. It has already been shown that intrinsic proteins would have little effect on hydrocarbon chain order in membranes above the gel to liquid−crystal phase transition temperature (T_c) of the pure lipids, at least in the time scale of ^{2}H NMR (*61*).

DISCUSSION

In this study, we present results suggesting that the lipid composition of the membrane modulates the mode in which Bak-C and Bcl-2-C insert into the membrane and the secondary structure that they adopt.

The study of the secondary structure of both domains reveals that their insertion in some membranes (such as DMPC, POPG, or POPC) increases the proportion of α-helix with both peptides and decreases the proportion of *β*-pleated sheet in the case of Bak-C or aggregated extended structures in the case of Bcl-2-C. These two last kinds of structure were very important when the peptides were in solution. On the other hand, when the peptides were incorporated in certain membranes (such as EYPC or OMM), the increase in α-helix content and the decrease in *β*-pleated sheet content (Bak-C) or aggregated extended structure (Bcl-2-C) were not so pronounced. It is noteworthy that, in general, the presence of cholesterol increases the likelihood that the peptides remain in *β*-pleated sheet (Bak-C) or aggregated extended structure (Bcl-2-C).

It is interesting that the negative charge of the lipids was not important in this context, as the secondary structure of both peptides in the presence of POPG was more similar to

that in DMPC vesicles than that in EYPC vesicles. In this sense, the composition of the fatty acyl chains (saturation degree and chain length) of the phospholipids may be important in determining the peptide structure. Note that the fatty acyl composition of the EYPC used was 16:0 (34.0%), 16:1 (1.7%), 18:0 (11.0%), 18:1 (32.0%), 18:2 (18.0%), and 20:4 (3.3%). In the presence of a membrane formed by DMPC which bears short fatty acyl chains, the peptide will match the hydrophobic thickness of the membrane and will adopt a predominantly α-helical structure, which will be nearly perpendicular to the plane of the lipid bilayer, as shown by ATR-IR. On the contrary, in the presence of lipids bearing longer fatty acyl chains and in the presence of cholesterol, the hydrophobic thickness of the membrane will be increased and a hydrophobic mismatch will appear so that the peptide will adopt a different secondary structure with the predominance of β-pleated sheet; the orientation with respect to the plane of the membrane will not be perpendicular, but instead, the helices will appear as disordered.

This suggestion is certainly supported by the changes observed in the secondary structure of Bak-C and by the ATR-IR study on the orientation of the α-helical component of the domain in the membrane. In this sense, the α-helix was observed to be clearly transmembranal, although slightly tilted with respect to the normal to the plane of the membrane (22°), in the case of DMPC membranes. However, in the presence of EYPC or OMM vesicles, Bak-C was not clearly oriented, since the result of 54° means that it is not possible to say whether this angle reflects the fact that there is a real tilt of 54° or that this is a mean of different orientations, indicating in this sense a certain degree of disorder or even the possibility that the peptide was partially or completely located outside the membrane.

The ATR-IR study of the orientation of the α-helical component of Bcl-2-C also confirms this interpretation since it is differently oriented, depending on membrane composition. In this sense, it is clearly oriented nearly perpendicular to the plane of the membrane in the case of DMPC membranes, with a maximum tilting angle of 10° with respect to the normal to this plane. However, in the case of OMM, the angle was 49° and in the presence of EYPC membranes it was 46°, indicating again disorder and a possibly superficial location of Bcl-2-C.

In conclusion, the fatty acyl chain composition (in both saturation degree and chain length) and the presence or absence of cholesterol produced different structures in both peptides, with different β-pleated sheet contents (in the case of Bak-C) or aggregated extended structures (in the case of Bcl-2-C), and α-helix. Taking into account these observations, we know Bak-C may have a different location or organization in the membrane, depending on the lipid composition, and we suggest that hydrophobic matching may be the key factor in determining the peptide's organization. In the case of Bcl-2-C, this interpretation seems to be valid because the presence of longer fatty acyl chains and cholesterol favors a more disordered or superficial location of the domain.

It should be mentioned at this point that the area of the amide I′ band varies from one sample to another. Taking into account the sample preparation procedure (see the Experimental Procedures) and the fact that only the lipid phase was loaded onto the FT-IR windows so that only the peptide bound to lipid is being measured, we determined it is possible that different lipid mixtures might have a preference for adsorbing peptides with a certain secondary structure. This interpretation should be taken as an alternative to the conclusion that certain lipid mixtures induce secondary structural changes.

The ^{2}H NMR study is also compatible with the conclusion concerning the transmembrane disposition of both Bak-C and Bcl-2-C in DMPC membranes, since it indicates a broadening of the phase transition but no change in the order parameter values. It is noteworthy that both peptides were well-oriented in the presence of DMPC vesicles, where they exhibited a high α-helix content and the lowest values of β-pleated sheet content (in the case of Bak-C) and aggregated extended structures (in the case of Bcl-2-C). With the rest of the lipid mixtures, higher β-pleated sheet contents and aggregated extended structures were observed, as seen by FT-IR, and in addition, a certain disorder was observed from the ATR-IR data. These results suppose that the penetration of both peptides in the membrane is probably related to the thickness of the membrane.

It is interesting to mention here some data determined experimentally with respect to the hydrophobic thickness of membranes as a function of lipid composition. The thickness of the hydrocarbon region of a DMPC bilayer in the liquid−crystalline phase was calculated as 2.3 nm using X-ray diffraction (*62*), which is in perfect agreement with the theorethical value of 2.28 nm obtained with the equation given by Sperotto and Mouritsen (*63*) [$d = 1.75(n - 1)$, where n is the number of carbon atoms of the fatty acyl chain]. In the case of POPC, the bilayer thickness in the fluid state was estimated to be 2.58 nm using ^{2}H NMR (*64*), whereas for an EYPC bilayer, it was 2.75 nm as seen through X-ray diffraction (*65*). The addition of cholesterol produces an increase in the hydrophobic thickness of the membrane; therefore, the addition of 50 mol % cholesterol to DMPC produced a bilayer thickness of 2.61 nm (*66*), and the presence of 30 mol % cholesterol in POPC increased the bilayer thickness from 2.58 to 2.99 nm (*64*). There are, then, clear quantitative differences between the thicknesses of the membranes under consideration.

Several reports can be found in the literature where the lipid composition of the membrane has been associated with the location and structure of membrane peptides and proteins. Hydrophobic matching between peptide and hydrophobic thickness has been associated with the degree of spontaneous insertion of a single spanning membrane protein (*67*). The presence of cholesterol, in particular, has been associated with a lower degree of penetration into the membrane of several synthetic peptides designed as transmembrane α-helices due to the increase in the hydrophobic thickness (*20*, *21*, *68*).

Given that Bak-C has a maximum α-helical percentage of 58% (in a DMPC membrane) and that its length is 24 amino acyl residues, 14 residues must be present in this conformation, and assuming 0.15 nm/residue for the α-helical conformation, the length will be 2.1 nm. Since the bilayer thickness of DMPC can be assumed to be 2.28 nm in a fluid bilayer (*62*, *63*), this means that Bak-C forms an α-helix stretch which totally spans the DMPC bilayer. In fact, the α-helix will be 0.18 nm shorter, i.e., approximately one residue, and it can be assumed that ∼50% of the first and

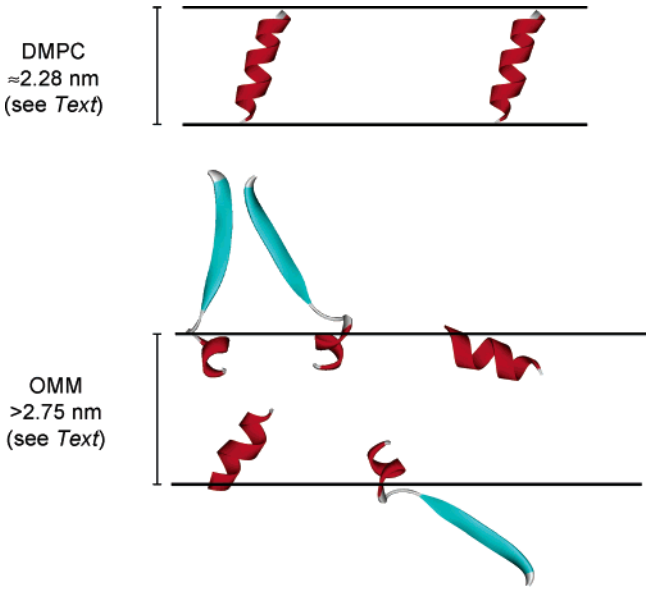

FIGURE 8: Schematic representation of the orientation of Bak-C or Bcl-2-C in a DMPC or OMM model membrane.

last residues of the α-helix are introduced in the hydrophobic part of the membrane (see Figure 8). We may assume that Bak-C adopts the same structure in POPC, POPG, and DMPC/EYPE-t membranes as in pure DMPC. In DMPC/cholesterol membranes (4:1 molar ratio), the hydrophobic thickness is slightly increased, and since the α-helical percentage is not altered, it can be concluded that Bak-C forms the same α-helical stretch that it does in the absence of cholesterol.

In the case of Bcl-2, the α-helical percentage in a DMPC membrane is 65%, and since it spans 23 residues, this means that 15 residues form the α-helix, with a length of 2.25 nm, which is very close to the length of 2.28 nm assumed above for a fluid bilayer of DMPC (*62*, *63*) (see Figure 8).

In the OMM, where Bak and Bcl-2 are assumed to insert their C-terminal domains, we have demonstrated that the hydrophobic thickness of the lipid is sufficient to produce a secondary structure of the peptides that will not include an α-helical stretch long enough to span the membrane. The reduced α-helical stretch will not be oriented within the membrane, and at least a portion of the peptide will probably be outside the membrane (see Figure 8). If this can be extrapolated to the full proteins, these C-terminal domains will not be transmembrane α-helices but will be only partially in this conformation and not oriented perpendicular to the plane of the membrane. In any case, it cannot be ruled out that some experimental results might be very different if the experiments are repeated with full-length proteins.

Hence, it will be necessary to experimentally test the assumption made up to now that the C-terminal domains of proteins such as Bcl-2 and Bak, which are thought to act by permanently anchoring them to the OMM, will adopt an α-helical structure or other secondary structures.

SUPPORTING INFORMATION AVAILABLE

FT-IR spectra of Bak-C in D_2O buffer at 20 °C (Figure 1), FT-IR spectra of Bcl-2-C in D_2O buffer at 20 °C (Figure 2), and control experiments with lower peptide:lipid molar ratios and with the acetylated form of Bcl-2-C in D_2O buffer at 20 °C (Figure 3). This material is available free of charge via the Internet at http://pubs.acs.org.

REFERENCES

1. Adams, J. M., and Cory, S. (1998) The Bcl-2 protein family: Arbiters of cell survival, *Science 281*, 1322−1326.
2. Adams, J. M., and Cory, S. (2001) Life-or-death decisions by the Bcl-2 protein family, *Trends Biochem. Sci. 26*, 61−66.
3. Chan, S. L., and Yu, V. C. (2004) Proteins of the Bcl-2 family in apoptosis signalling: From mechanistic insights to therapeutic opportunities, *Clin. Exp. Pharmacol. Physiol. 31*, 119−128.
4. Tsujimoto, Y., and Shimizu, S. (2000) Bcl-2 family: Life-or-death switch, *FEBS Lett. 466*, 6−10.
5. Sattler, M., Liang, H., Nettesheim, D., Meadows, R. P., Harlan, J. E., Eberstadt, M., Yoon, H. S., Shuker, S. B., Chang, B. S., Minn, A. J., Thompson, C. B., and Fesik, S. W. (1997) Structure of Bcl-x_L-Bak peptide complex: Recognition between regulators of apoptosis, *Science 275*, 983−986.
6. Opferman, J. T., and Korsmeyer, S. J. (2003) Apoptosis in the development and maintenance of the immune system, *Nat. Immunol. 4*, 410−415.
7. Huang, D. C., and Strasser, A. (2000) BH3-only proteins: Essential initiators of apoptotic cell death, *Cell 103*, 839−842.
8. Schendel, S. L., Montal, M., and Reed, J. C. (1998) Bcl-2 family proteins as ion-channels, *Cell Death Differ. 5*, 372−380.
9. Nguyen, M., Millar, D. G., Yong, V. W., Korsmeyer, S. J., and Shore, G. C. (1993) Targeting of Bcl-2 to the mitochondrial outer membrane by a COOH-terminal signal anchor sequence, *J. Biol. Chem. 268*, 25265−25268.
10. Janiak, F., Leber, B., and Andrews, D. W. (1994) Assembly of Bcl-2 into microsomal and outer mitochondrial membranes, *J. Biol. Chem. 269*, 9842−9849.
11. Clow, A., Greenhalf, W., and Chaudhuri, B. (1998) Under respiratory growth conditions, Bcl-x(L) and Bcl-2 are unable to overcome yeast cell death triggered by a mutant Bax protein lacking the membrane anchor, *Eur. J. Biochem. 258*, 19−28.
12. Priault, M., Camougrand, N., Chaudhuri, B., and Manon, S. (1999) Role of the C-terminal domain of Bax and Bcl-xL in their localization and function in yeast cells, *FEBS Lett. 443*, 225−228.
13. del Mar Martinez-Senac, M., Corbalan-Garcia, S., and Gomez-Fernandez, J. C. (2000) Study of the secondary structure of the C-terminal domain of the antiapoptotic protein Bcl-2 and its interaction with model membranes, *Biochemistry 39*, 7744−7752.
14. Hinds, M. G., Lackmann, M., Skea, G. L., Harrison, P. J., Huang, D. C., and Day, C. L. (2003) The structure of Bcl-w reveals a role for the C-terminal residues in modulating biological activity, *EMBO J. 22*, 1497−1507.
15. Priault, M., Camougrand, N., Kinnally, K. W., Vallette, F. M., and Manon, S. (2003) Yeast as a tool to study Bax/mitochondrial interactions in cell death, *FEMS Yeast Res. 4*, 15−27.
16. Scorrano, L., and Korsmeyer, S. J. (2003) Mechanisms of cytochrome *c* release by proapoptotic Bcl-2 family members, *Biochem. Biophys. Res. Commun. 304*, 437−444.
17. Martinez-Senac, M. M., Corbalan-Garcia, S., and Gomez-Fernandez, J. C. (2002) The structure of the C-terminal domain of the pro-apoptotic protein Bak and its interaction with model membranes, *Biophys. J. 82*, 233−243.
18. Prenner, E. J., Lewis, R. N., Jelokhani-Niaraki, M., Hodges, R. S., and McElhaney, R. N. (2001) Cholesterol attenuates the interaction of the antimicrobial peptide gramicidin S with phospholipid bilayer membranes, *Biochim. Biophys. Acta 1510*, 83−92.
19. Gorbenko, G., Handa, T., Saito, H., Molotkovsky, J., Tanaka, M., Egashira, M., and Nakano, M. (2003) Effect of cholesterol on bilayer location of the class A peptide Ac-18A-NH2 as revealed by fluorescence resonance energy transfer, *Eur. Biophys. J. 32*, 703−709.
20. Ren, J., Lew, S., Wang, Z., and London, E. (1997) Transmembrane orientation of hydrophobic α-helices is regulated both by the relationship of helix length to bilayer thickness and by the cholesterol concentration, *Biochemistry 36*, 10213−10220.
21. Curtain, C. C., Ali, F. E., Smith, D. G., Bush, A. I., Masters, C. L., and Barnham, K. J. (2003) Metal ions, pH, and cholesterol regulate the interactions of Alzheimer's disease amyloid-β peptide with membrane lipid, *J. Biol. Chem. 278*, 2977−2982.

22. Epand, R. M., Epand, R. F., Sayer, B. G., Datta, G., Chaddha, M., and Anantharamaiah, G. M. (2004) Two homologous apolipoprotein AI mimetic peptides. Relationship between membrane interactions and biological activity, *J. Biol. Chem. 279*, 51404−51414.
23. Nicol, F., Nir, S., and Szoka, F. C., Jr. (1996) Effect of cholesterol and charge on pore formation in bilayer vesicles by a pH-sensitive peptide, *Biophys. J. 71*, 3288−3301.
24. Kyte, J., and Doolittle, R. F. (1982) A rapid method for displaying the hydropathic character of a protein, *J. Mol. Biol. 157*, 105−132.
25. Hsu, S. Y., Kaipia, A., McGee, E., Lomeli, M., and Hsueh, A. J. (1997) Bok is a pro-apoptotic Bcl-2 protein with restricted expression in reproductive tissues and heterodimerizes with selective anti-apoptotic Bcl-2 family members, *Proc. Natl. Acad. Sci. U.S.A. 94*, 12401−12406.
26. Petros, A. M., Medek, A., Nettesheim, D. G., Kim, D. H., Yoon, H. S., Swift, K., Matayoshi, E. D., Oltersdorf, T., and Fesik, S. W. (2001) Solution structure of the antiapoptotic protein Bcl-2, *Proc. Natl. Acad. Sci. U.S.A. 98*, 3012−3017.
27. Kaufmann, T., Schlipf, S., Sanz, J., Neubert, K., Stein, R., and Borner, C. (2003) Characterization of the signal that directs Bcl-x(L), but not Bcl-2, to the mitochondrial outer membrane, *J. Cell Biol. 160*, 53−64.
28. Del Mar Martinez-Senac, M., Corbalan-Garcia, S., and Gomez-Fernandez, J. C. (2001) Conformation of the C-terminal domain of the pro-apoptotic protein Bax and mutants and its interaction with membranes, *Biochemistry 40*, 9983−9992.
29. Torrecillas, A., Corbalan-Garcia, S., and Gomez-Fernandez, J. C. (2003) Structural study of the C2 domains of the classical PKC isoenzymes using infrared spectroscopy and two-dimensional infrared correlation spectroscopy, *Biochemistry 42*, 11669−11681.
30. Torrecillas, A., Corbalan-Garcia, S., and Gomez-Fernandez, J. C. (2004) An infrared spectroscopic study of the secondary structure of protein kinase C α and its thermal denaturation, *Biochemistry 43*, 2332−2344.
31. Arrondo, J. L. R., Muga, A., Castresana, J., Bernabeu, C., and Goñi, F. M. (1989) An infrared spectroscopic study of β-galactosidase structure in aqueous solutions, *FEBS Lett. 252*, 118−120.
32. Arrondo, J. L., Castresana, J., Valpuesta, J. M., and Goñi, F. M. (1994) Structure and thermal denaturation of crystalline and noncrystalline cytochrome oxidase as studied by infrared spectroscopy, *Biochemistry 33*, 11650−11655.
33. Goormaghtigh, E., Cabiaux, V., and Ruysschaert, J. M. (1994) Determination of soluble and membrane protein structure by Fourier transform infrared spectroscopy. III. Secondary structures, *Subcell. Biochem. 23*, 405−450.
34. Goormaghtigh, E., Raussens, V., and Ruysschaert, J. M. (1999) Attenuated total reflection infrared spectroscopy of proteins and lipids in biological membranes, *Biochim. Biophys. Acta 1422*, 105−185.
35. Vigano, C., Manciu, L., Buyse, F., Goormaghtigh, E., and Ruysschaert, J. M. (2000) Attenuated total reflection IR spectroscopy as a tool to investigate the structure, orientation and tertiary structure changes in peptides and membrane proteins, *Biopolymers 55*, 373−380.
36. Goormaghtigh, E., Cabiaux, V., and Ruysschaert, J. M. (1994) Determination of soluble and membrane protein structure by Fourier transform infrared spectroscopy. I. Assignments and model compounds, *Subcell. Biochem. 23*, 329−362.
37. Marsh, D., Muller, M., and Schmitt, F. J. (2000) Orientation of the infrared transition moments for an α-helix, *Biophys. J. 78*, 2499−2510.
38. Bechinger, B., Ruysschaert, J. M., and Goormaghtigh, E. (1999) Membrane helix orientation from linear dichroism of infrared attenuated total reflection spectra, *Biophys. J. 76*, 552−563.
39. Fringeli, U. P., and Gunthard, H. H. (1981) Infrared membrane spectroscopy, *Mol. Biol. Biochem. Biophys. 31*, 270−332.
40. Davis, D. G., Inesi, G., and Gulik-Krzywicki, T. (1976) Lipid molecular motion and enzyme activity in sarcoplasmic reticulum membrane, *Biochemistry 15*, 1271−1276.
41. Sternin, E., Bloom, M., and MacKay, A. L. (1983) DePake-ing of NMR spectra, *J. Magn. Reson. 55*, 274−282.
42. Krimm, S., and Bandekar, J. (1986) Vibrational spectroscopy and conformation of peptides, polypeptides, and proteins, *Adv. Protein Chem. 38*, 181−364.
43. Susi, H., and Byler, D. M. (1987) Fourier transform infrared study of proteins with parallel β-chains, *Arch. Biochem. Biophys. 258*, 465−469.
44. Arrondo, J. L., Muga, A., Castresana, J., and Goni, F. M. (1993) Quantitative studies of the structure of proteins in solution by Fourier transform infrared spectroscopy, *Prog. Biophys. Mol. Biol. 59*, 23−56.
45. Arrondo, J. L., and Goni, F. M. (1999) Structure and dynamics of membrane proteins as studied by infrared spectroscopy, *Prog. Biophys. Mol. Biol. 72*, 367−405.
46. Fabian, H., Naumann, D., Misselwitz, R., Ristau, O., Gerlach, D., and Welfle, H. (1992) Secondary structure of streptokinase in aqueous solution: A Fourier transform infrared spectroscopic study, *Biochemistry 31*, 6532−6538.
47. Muga, A., Arrondo, J. L., Bellon, T., Sancho, J., and Bernabeu, C. (1993) Structural and functional studies on the interaction of sodium dodecyl sulfate with β-galactosidase, *Arch. Biochem. Biophys. 300*, 451−457.
48. Gonzalez, M., Bagatolli, L. A., Echabe, I., Arrondo, J. L., Argarana, C. E., Cantor, C. R., and Fidelio, G. D. (1997) Interaction of biotin with streptavidin. Thermostability and conformational changes upon binding, *J. Biol. Chem. 272*, 11288−11294.
49. Bandekar, J., and Krimm, S. (1980) Vibrational analysis of peptides, polypeptides, and proteins. VI. Assignment of β-turn modes in insulin and other proteins, *Biopolymers 19*, 31−36.
50. Clark, A. H., Saunderson, D. H., and Suggett, A. (1981) Infrared and laser-Raman spectroscopic studies of thermally-induced globular protein gels, *Int. J. Pept. Protein Res. 17*, 353−364.
51. Haltia, T., Semo, N., Arrondo, J. L., Goni, F. M., and Freire, E. (1994) Thermodynamic and structural stability of cytochrome *c* oxidase from *Paracoccus denitrificans*, *Biochemistry 33*, 9731−9740.
52. Yang, P. W., Stewart, L. C., and Mantsch, H. H. (1987) Polarized attenuated total reflectance spectra of oriented purple membranes, *Biochem. Biophys. Res. Commun. 145*, 298−302.
53. Seelig, A., and Seelig, J. (1980) Lipid conformation in model membranes and biological membranes, *Q. Rev. Biophys. 13*, 19−61.
54. Frey, S., and Tamm, L. K. (1991) Orientation of melittin in phospholipid bilayers. A polarized attenuated total reflection infrared study, *Biophys. J. 60*, 922−930.
55. Goormaghtigh, E., De Meutter, J., Szoka, F., Cabiaux, V., Parente, R. A., and Ruysschaert, J. M. (1991) Secondary structure and orientation of the amphipathic peptide GALA in lipid structures. An infrared-spectroscopic approach, *Eur. J. Biochem. 195*, 421−429.
56. Goormaghtigh, E., Cabiaux, V., and Ruysschaert, J. M. (1990) Secondary structure and dosage of soluble and membrane proteins by attenuated total reflection Fourier-transform infrared spectroscopy on hydrated films, *Eur. J. Biochem. 193*, 409−420.
57. Davis, J. H. (1983) The description of membrane lipid conformation, order and dynamics by ^{2}H NMR, *Biochim. Biophys. Acta 737*, 117−171.
58. Burnett, L., and Muller, B. H. (1971) Deuterium quadrupole coupling constants in three solid deuterated paraffin hydrocarbons C2D6, C4D10, C6D14, *J. Chem. Phys. 55*, 5829−5831.
59. Seelig, J. (1977) Deuterium magnetic resonance: Theory and application to lipid membranes, *Q. Rev. Biophys. 10*, 353−418.
60. Davis, J. H. (1979) Deuterium magnetic resonance study of the gel and liquid crystalline phases of dipalmitoyl phosphatylcholine, *Biophys. J. 27*, 339−358.
61. Rice, D. M., Meadows, M. D., Scheinman, A. O., Goni, F. M., Gomez-Fernandez, J. C., Moscarello, M. A., Chapman, D., and Oldfield, E. (1979) Protein−lipid interactions. A nuclear magnetic resonance study of sarcoplasmic reticulum Ca^{2+},Mg^{2+}-ATPase, lipophilin, and proteolipid apoprotein-lecithin systems and a comparison with the effects of cholesterol, *Biochemistry 18*, 5893−5903.
62. Lewis, B. A., and Engelman, D. M. (1983) Lipid bilayer thickness varies linearly with acyl chain length in fluid phosphatidylcholine vesicles, *J. Mol. Biol. 166*, 211−217.
63. Sperotto, M. M., and Mouritsen, O. G. (1988) Dependence of lipid membrane phase transition temperature on the mismatch of protein and lipid hydrophobic thickness, *Eur. Biophys. J. 16*, 1−10.

64. Nezil, F. A., and Bloom, M. (1992) Combined influence of cholesterol and synthetic amphiphillic peptides upon bilayer thickness in model membranes, *Biophys. J. 61*, 1176−1183.
65. Klose, G., König, B., Gordeliy, V. I., and Schulze, G. (1991) Incorporation of phosphonic acid diesters into lipid model membranes. Part II. X-ray and neutron diffraction studies, *Chem. Phys. Lipids 59*, 137−149.
66. Needham, D., McIntosh, T. J., and Evans, E. (1988) Thermomechanical and transition properties of dimyristoylphosphatidylcholine/cholesterol bilayers, *Biochemistry 27*, 4668−4673.
67. Ridder, A. N., van de Hoef, W., Stam, J., Jun, A., de Kruijff, B., and Killian, J. A. (2002) Importance of hydrophobic matching for spontaneous insertion of a single-spanning membrane protein, *Biochemistry 41*, 4946−4952.
68. Webb, R. J., East, J. M., Sharma, R. P., and Lee, A. G. (1998) Hydrophobic mismatch and the incorporation of peptides into lipid bilayers: A possible mechanism for retention in the Golgi, *Biochemistry 37*, 673−679.

BI0503192